

HyperVQ: MLR-based Vector Quantization in Hyperbolic Space

Nabarun Goswami¹, Yusuke Mukuta^{1,2}, and Tatsuya Harada^{1,2}

¹ The University of Tokyo, Japan

² RIKEN, Japan

{nabarungoswami,mukuta,harada}@mi.t.u-tokyo.ac.jp

Abstract. The success of models operating on tokenized data has led to an increased demand for effective tokenization methods, particularly when applied to vision or auditory tasks, which inherently involve non-discrete data. One of the most popular tokenization methods is Vector Quantization (VQ), a key component of several recent state-of-the-art methods across various domains. Typically, a VQ Variational Autoencoder (VQVAE) is trained to transform data to and from its tokenized representation. However, since the VQVAE is trained with a reconstruction objective, there is no constraint for the embeddings to be well disentangled, a crucial aspect for using them in discriminative tasks. Recently, several works have demonstrated the benefits of utilizing hyperbolic spaces for representation learning. Hyperbolic spaces induce compact latent representations due to their exponential volume growth and inherent ability to model hierarchical and structured data. In this work, we explore the use of hyperbolic spaces for vector quantization (HyperVQ), formulating the VQ operation as a hyperbolic Multinomial Logistic Regression (MLR) problem, in contrast to the Euclidean K-Means clustering used in VQVAE. Through extensive experiments, we demonstrate that HyperVQ performs comparably in reconstruction and generative tasks while outperforming VQ in discriminative tasks and learning a highly disentangled latent space.

Keywords: Hyperbolic Neural Networks · Vector Quantization

1 Introduction

Tokenization has become an essential step in numerous data processing pipelines with the surge of transformer-based models applied to diverse tasks and domains. While tokenizing discrete data like text is straightforward, continuous data types such as images or audio demand a distinct approach.

Typically, to discretize data, a VQVAE [35] is employed, and the resulting discrete tokens serve as input for training other token-based models. The choice of tokenization method significantly influences the model’s performance, depending on the task. For instance, tokens trained with reconstruction objectives excel in generative tasks such as VQVAE [35] and soundstream [37], where the goal is to reconstruct input or generate new samples. In contrast, discriminative tasks like

quality-independent representation learning for robust image classification [36] or learning semantic speech representations [3] utilize a discriminative objective, guiding tokens to be less redundant and more discriminative. Additionally, disentangled features simplify the learning process for other models built on top of tokenized representations. In this work, we explore a disentangled tokenization method suitable for both generative and discriminative tasks.

Recent trends highlight the advantages of learning representations in non-Euclidean spaces, especially the capability of hyperbolic spaces to naturally represent hierarchical data and induce compact embeddings due to exponential volume growth with radius. Hyperbolic representations are known for better generalization, less overfitting, reduced computational complexity, lower data requirements, and preservation of local and geometric information [26]. Several works have explored hyperbolic spaces for learning text representations [23], images [1, 15], audio [27], etc., demonstrating advantages over Euclidean counterparts.

In this work, we harness the properties of hyperbolic spaces to develop a robust and efficient tokenization method. We propose formulating the nearest neighbor search problem in VQ as a multinomial logistic regression in hyperbolic space, with quantized vectors serving as representative points of hyperbolic decision hyperplanes. Our approach, HyperVQ, differs from Gumbel Vector quantization (GumbelVQ) [2], which predicts codebook vector indices and is trained using the straight-through estimator [4]. The key distinctions lie in our choice of the latent space and the selection of representative points as codebook vectors, rather than optimizing a separate codebook matrix. The hyperbolic MLR formulation encourages embeddings to be highly localized within regions enclosed by decision hyperplanes, thus inducing implicit disentanglement of the latent space. Moreover, selecting a representative point on the decision hyperplane as the codebook vector enhances robustness to noise and outliers, ensuring a stable training process less dependent on codebook vector initialization. Experimental results validate that the proposed method improves the discriminative performance of tokenization while maintaining generative performance.

The contributions of this work are summarized as follows:

- First realization, to the best of our knowledge, of a vector quantization method, a key building block of modern deep learning architectures, for hyperbolic spaces.
- Definition of geometrically constrained codebook vectors, leading to enhanced disentanglement and compact latent representations.
- Demonstration of HyperVQ’s ability to improve discriminative performance while maintaining generative performance.

2 Related Work

2.1 Discrete Representation Learning

Discrete representation of data is essential for various purposes, including compression and tokenization. While vector quantization [10] has been a critical

component of classical signal processing methods, it has gained significant traction in the deep learning community. First proposed in [35], the VQVAE applies vector quantization to the latent space of a VAE, transitioning from a continuous to a discrete latent space. This approach offers advantages, such as learning powerful priors on the discrete space, as demonstrated by pixelCNN [24].

More recently, tokenized image synthesis methods like VQGAN [8], VQGAN+CLIP [5], and VQ-Diffusion [11] have shown impressive results in image generation. While discrete representation has excelled in generative tasks, vector quantization has also been integrated into discriminative tasks. For instance, Yang et al. [36] proposed combining quantized representation with unquantized ones for quality-independent representation learning, and Lu et al. [21] introduced a hierarchical vector quantized transformer for unsupervised anomaly detection. Vector quantization’s applicability extends beyond computer vision to domains such as audio [2, 3, 37].

While several works have explored enhancing vector quantization operations to address issues like index collapse [19, 29, 34], to the best of our knowledge, no work has explored simultaneously improving the generative and discriminative capabilities of quantized representations.

2.2 Hyperbolic Deep Learning

Non-Euclidean geometry offers a promising approach to uncover inherent geometrical structures in high-dimensional data. Hyperbolic spaces, known for their exponential volume growth with respect to radius, induce low-distortion embeddings and provide better model interpretation [26]. Hyperbolic embeddings exhibit robustness to noise and outliers and demonstrate better generalization capabilities with reduced overfitting, computational complexity, and data requirements [15, 23].

Various works, including [9, 32], lay the mathematical foundation for creating neural networks in hyperbolic space. Building upon these foundations, methods have been proposed to address tasks such as image segmentation [1], audio source separation [27], image-text representation learning [7], and variational autoencoders [22, 33].

While a solid foundation of hyperbolic neural network building blocks have been laid, there still lacks a principled and effective vector quantization method utilizing the hyperbolic space. Since VQ is such an important mechanism of several modern neural network architectures across domains. In this work, we explore the definition of a VQ method for the hyperbolic space which can improve feature disentanglement while maintaining the geometric properties of the quantized latents.

3 Preliminaries

In this section, we provide a concise overview of non-Euclidean geometry and relevant theories crucial for understanding the foundations of our work. While

we touch upon the basics, for an in-depth exploration, we recommend referring to [9]. Additionally, we introduce the concepts of vector quantization and vector quantized variational autoencoders, laying the groundwork for the subsequent discussions.

3.1 Hyperbolic Geometry

Riemannian Manifold A manifold is a n -dimensional topological space \mathcal{M} , such that $\forall x \in \mathcal{M}$, the tangent space, $\mathcal{T}_x\mathcal{M}$ of \mathcal{M} at x , can be approximated by \mathbb{R}^n . A manifold paired with a group of Riemannian metric tensors, $g_x : \mathcal{T}_x\mathcal{M} \times \mathcal{T}_x\mathcal{M} \rightarrow \mathbb{R}^n$, is called a Riemannian manifold (\mathcal{M}, g) .

Hyperbolic Space and Poincaré Ball Model A Riemannian manifold is called a hyperbolic space if its sectional curvature is negative everywhere. There are several models to represent the n -dimensional hyperbolic space with constant negative curvature, such as the Hyperboloid model, the Poincaré ball model, the Beltrami-Klein model, etc.

In this work, we use the Poincaré ball model, which is defined by the pairing of the manifold $\mathbb{P}_c^n = \left\{ x \in \mathbb{R}^n \mid \|x\| < \frac{1}{\sqrt{c}} \right\}$ and the metric

$g_x^{\mathbb{P}} = \lambda_x^2 g_x^{\mathbb{R}^n}$ where c is the radius of the ball, $g_x^{\mathbb{R}^n}$ is the Euclidean metric on \mathbb{R}^n and $\lambda_x = 2(1 - \|x\|^2)^{-1}$ is called the conformal factor between the two metrics. Two metrics are conformal if they define the same angles.

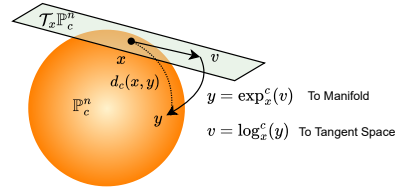


Fig. 1: Illustration of the Poincaré ball model and its associated exponential and logarithmic maps

Gyrovector Spaces and Poincaré Operations Gyrovector spaces provide an algebraic structure to the hyperbolic space, which is analogous to the vector space structure of the Euclidean space. Several operations on the Poincaré ball model \mathbb{P}_c^n are defined under this framework such as Möbius addition \oplus_c , distance between points on the manifold $d_c(x, y)$, exponential and logarithmic maps. We refer the reader to [9] for a detailed explanation of these operations. Here we present the definitions of the exponential and logarithmic maps which are pertinent to our work. The following operations are defined under the framework of gyrovector spaces and considering the Poincaré ball model \mathbb{P}_c^n :

$$\exp_x^c(v) = x \oplus_c \left(\tanh \left(\sqrt{c} \frac{\lambda_x \|v\|}{2} \right) \frac{v}{\sqrt{c} \|v\|} \right) \quad (1)$$

$$\log_x^c(y) = \frac{2}{\sqrt{c} \lambda_x} \tanh^{-1} \left(\sqrt{c} \|-x \oplus_c y\| \right) \frac{-x \oplus_c y}{\|-x \oplus_c y\|} \quad (2)$$

The exponential and logarithmic maps allow us to move between the tangent space (Euclidean) and the manifold as shown in Fig. 1.

Poincaré Hyperplanes, MLR and Unidirectional MLR In [9], the authors generalized the concept of a hyperplane in Euclidean space to hyperbolic space, by defining it as the set of all geodesics containing an arbitrary point $p \in \mathbb{P}_c^n$ and orthogonal to a tangent vector $a \in \mathcal{T}_p \mathbb{P}_c^n \setminus \{\mathbf{0}\}$.

$$H_{a,p}^c = \{x \in \mathbb{P}_c^n : \langle -p \oplus_c x, a \rangle = 0\} \quad (3)$$

However, as shown in [32], this definition causes over-parameterization of the hyperplane. They instead proposed an unidirectional hyperplane formulation by fixing the choice of the point on the manifold to be parallel to the normal vector. This is done by introducing a new scalar parameter $r_k \in \mathbb{R}$ which allows the definition of the bias vector in terms of r_k and the normal vector a_k , as,

$$q_k = \exp_0^c(r_k[a_k]) \quad (4)$$

and correspondingly, the hyperplane can be defined in terms of q_k as,

$$\bar{H}_{a_k, r_k}^c := \{x \in \mathbb{P}_c^n \mid \langle -q_k \oplus_c x, a_k \rangle = 0\} \quad (5)$$

Following this new formulation, the hyperbolic multinomial logistic regression (MLR), which is a generalization of the Euclidean MLR formulation (from the perspective of distances to margin hyperplanes), to perform classification tasks in hyperbolic space was defined. The unidirectional hyperbolic MLR formulation given K classes, $k \in \{1, 2, \dots, K\}$ and for all $x \in \mathbb{P}_c^n$ is defined as follows:

$$\begin{aligned} v_k &= p(y = k \mid x) \\ &\propto \text{sign}(\langle -q_k \oplus_c x, a_k \rangle) \|a_k\| d_c(z_h, \bar{H}_{a_k, r_k}^c) \end{aligned} \quad (6)$$

3.2 Vector Quantization and VQVAE

Vector Quantization (VQ) is a data compression and signal processing technique that approximates a continuous input signal $z_e \in \mathbb{R}^N$ by mapping it to the nearest vector from a codebook $C = \{C_1, C_2, \dots, C_K\}$ of K codebook vectors. This mapping is defined as $k = q(z_e) = \arg \min_k \|z_e - C_k\|$, where k is the index of the nearest codebook vector, and the quantized approximation $\hat{z}_e = z_q = C_k$. VQ is crucial in image and speech compression, clustering, and quantization tasks, where it simplifies data while preserving essential information.

Building on the concept of VQ, the Vector Quantized Variational Autoencoder (VQVAE) introduces a discrete latent representation between the encoder and decoder stages of a Variational Autoencoder (VAE). The encoder outputs a continuous latent representation z_e , which is quantized into z_q using the VQ process for the decoder to reconstruct the input. To enable end-to-end training despite the non-differentiable nature of the quantization step, a straight-through

estimator is employed, allowing gradients to pass through. The loss function incorporates a commitment loss to ensure the encoder reliably maps inputs to specific codebook vectors:

$$L = \log p(x | z_q) + \|\text{sg}[z_e] - z_q\|_2^2 + \beta \|z_e - \text{sg}[z_q]\|_2^2 \quad (7)$$

Here, sg indicates the stop-gradient operation, and β balances the commitment loss. Further developments in VQVAE have explored alternative quantization strategies, such as using Gumbel Softmax [4] for codebook vector selection [2], enhancing the model’s flexibility and application range.

4 Method

We propose to formulate the Vector Quantization (VQ) operation as a multinomial logistic regression in hyperbolic space. To enhance the disentanglement of the codebook vectors, we suggest using the representative points of the decision hyperplanes as the codebook vectors, instead of learning a separate embedding matrix. Fig. 2 illustrates the overall pipeline of an encoder-decoder network with integrated HyperVQ. The encoder and decoder operate in Euclidean space, while vector quantization occurs in hyperbolic space. The architectures of the encoder and decoder can vary depending on the task at hand. Algorithm 1 presents task-agnostic pseudocode for training models with HyperVQ. In the following

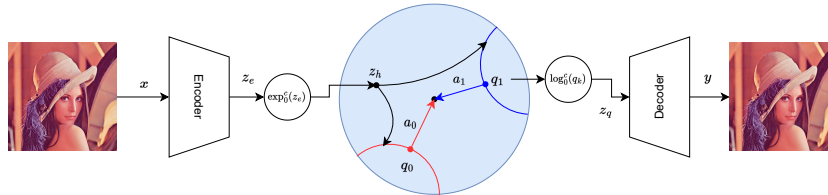


Fig. 2: Illustration of HyperVQ in a VQVAE setting. The key steps are the projection of the euclidean embeddings to the hyperbolic space, classification of the projected embeddings to one of K classes, and utilization of the representative point on the hyperplane, q_k as the codebook vector which is projected back to the Euclidean space.

subsections, we provide a detailed description of HyperVQ, followed by architecture descriptions tailored to different tasks.

4.1 HyperVQ

Projection The latent representation $z_e \in \mathbb{R}^d$ is projected onto the Poincaré ball \mathbb{P}_c^n using the exponential map \exp_0^c (Eq. (1)), which gives us the projected latent representation $z_h \in \mathbb{P}_c^n$. We also use the safe projection method suggested in [9],

$$z_h = \begin{cases} \frac{\exp_0^c(z_e)}{\|\exp_0^c(z_e)\|_2} \cdot \frac{1-\epsilon}{\sqrt{c}} & \text{if } \|\exp_0^c(z_e)\|_2 > \frac{1-\epsilon}{\sqrt{c}} \\ \exp_0^c(z_e) & \text{otherwise} \end{cases} \quad (8)$$

which prevents numerical instability when the norm of the projected latent representation is close to the boundary of the Poincaré ball.

4.2 Difficulty of Central Measure in Hyperbolic Spaces

Hyperbolic MLR for Vector Quantization Once we obtain the projected embeddings z_h , we need to map them to a codebook vector. In principle, we follow the Gumbel Vector Quantization [2] method to regress the logits for codebook vector selection. To accommodate the fact that our embeddings are projected onto the hyperbolic space, we perform hyperbolic multinomial logistic regression. The hyperplane formulation in Eq. (3) requires two n -dimensional parameters: an arbitrary bias vector p_k lying on the manifold \mathbb{P}_c^n and the normal vector a_k lying on its tangent space $\mathcal{T}_{p_k} \mathbb{P}_c^n$. Instead we use the unidirectional MLR as given in Eq. (5), which has several advantages. Firstly, it reduces the number of parameters from $2n$ to $n+1$. Secondly, it provides a way to succinctly capture all relevant information about the decision hyperplane using the bias vector on the manifold, q_k . Finally, since the parameter r_k is scalar, and a_k lies on the Euclidean tangent space, standard gradient optimization methods can be utilized for training.

This allows us to predict the logits and choose q_k as a fixed and single point representing each decision hyperplane. The logits from the MLR are converted to one-hot vectors using the Gumbel Softmax [14], and the gradients are passed through the quantization layer using the straight-through estimator [4].

Geometrically Constrained Codebook Vectors The choice of the codebook vector is crucial in training a vector quantized model. Typical choices include cluster centroids of online K-Means clustering in VQVAE or an embedding matrix in the case of Gumbel Vector Quantization (GumbelVQ). While cluster centroids from K-Means capture the underlying geometric properties of the latent space, the embedding matrix in case of GumbelVQ do not have such geometric properties and reconstruction objective tends to mold the vectors in a way that makes it easier to reconstruct the input.

However, central measure computations in hyperbolic space are not straightforward [20] and require expensive iterative computations. Also, as the vectors get closer to the boundary of the Poincaré ball, distances grow exponentially, which can create numerical instability due to limitations of floating point arithmetic in computers. Apart from that, neither of these choices incentivizes the codebook vectors to be disentangled.

Therefore, what we seek in a codebook vector is representation of the geometrical structure of embeddings assigned to it and disentanglement. One such

entity is q_k , a point on the manifold that uniquely represents both the position and orientation of each of the k decision hyperplanes. The added advantage of using the representative point of the decision hyperplanes is that they are naturally disentangled and are not influenced by outliers. Additionally, the decoder is forced to use these disentangled features for reconstruction, thereby retaining the high discriminative ability of the quantized features.

Since our decoder is Euclidean, we need to project q_k back to the Euclidean space, using the logarithmic map (Eq. (2)) and using Eq. (4), we have,

$$\begin{aligned} z_q &= \log_0^c(q_k) \\ &= \log_0^c(\exp_0^c(r_k[a_k])) \\ &= r_k[a_k] \end{aligned} \tag{9}$$

Thus, the codebook vector is the product of the normal vector a_k and the scalar parameter r_k .

Algorithm 1 HyperVQ Training

- 1: **Initialization:** Initial network parameters of Encoder (θ_E), Decoder (θ_D), and Quantizer ($\theta_Q = \{a_k, r_k\}$ for $k = 0, 1, \dots, K$) and temperature, $\tau \in [\tau_{\max}, \tau_{\min}]$, and decay factor δ
 - 2: **Training:**
 - 3: **for** each iteration, j **do**
 - 4: sample data, x
 - 5: $z_e = \text{Encoder}(x)$
 - 6: $z_h = \exp_0^c(z_e)$
 - 7: $\text{logits} = \text{unidirectional_mlr}(z_h)$ (Eq. (6))
 - 8: $k = \text{argmax}(\text{gumbel_softmax}(\text{logits}, \tau))$
 - 9: $z_q = r_k[a_k]$ (Eq. (9))
 - 10: $\tau = \max(\tau_{\max} \cdot \delta^j, \tau_{\min})$
 - 11: $y = \text{Decoder}(z_q)$
 - 12: Update $\theta_E, \theta_D, \theta_Q$ by gradient descent
 - 13: **end for**
-

4.3 Model Architectures

VQVAE We utilize the architecture depicted in Fig. 2 for the VQVAE. The encoder comprises an initial convolutional encoder block, followed by a stack of residual blocks, before being passed through the quantization layer. The decoder is the inverse of the encoder, with the residual blocks and the convolutional encoder block replaced by a transposed convolutional decoder block for upsampling. The quantization layer adopts the hyperbolic MLR formulation, as described in Sec. 4.1. The model is trained end-to-end using the mean squared error (MSE) loss between the input and the reconstructed output.

Classification We employ the pretrained VQVAE as the feature extractor for the classification task. The architecture is depicted in Fig. 3, where we utilize

a lightweight classifier consisting of a convolutional layer with ReLU activation, followed by a global average pooling layer and two fully connected layers to obtain the logits. Only the classifier block is trained using the cross-entropy loss, while keeping the parameters of the convolutional encoder, residual blocks, and the quantization layer fixed. Since we use the codebook vectors given by Eq. (9), we can directly implement the classifier in Euclidean space.

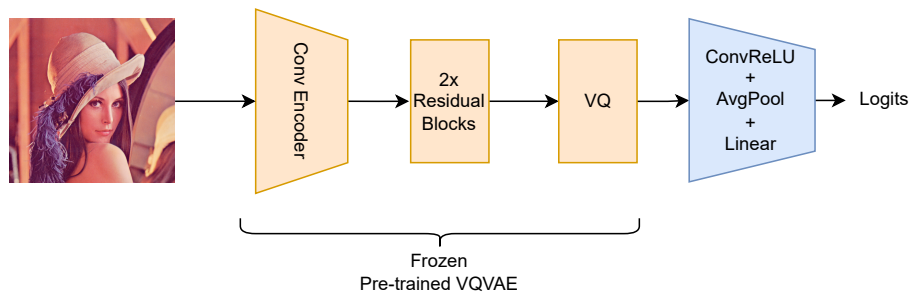


Fig. 3: Classification pipeline with pretrained VQVAE. The encoder and vector quantizer are pre-trained and kept frozen and only the classifier block is trained.

5 Experiments

To assess the effectiveness of our proposed method, we conducted experiments across diverse tasks, encompassing image reconstruction, generative modeling, image classification, and feature disentanglement. The implementation details and results of each experiment are elaborated upon in the following subsections.

5.1 Implementation Details

Our method was implemented using the PyTorch library [25]. Model training was conducted on 4 A100 GPUs utilizing the Adam optimizer [16], with a learning rate set at $3e-4$ and a batch size of 128 per GPU, unless otherwise specified. For hyperbolic functions, we employed the geopt library [17] and referenced the official implementation of hyperbolic neural networks++ [32].

5.2 Reconstruction and Generative Modeling

To assess the generative modeling capabilities of the proposed HyperVQ method, we conducted experiments on the Cifar100 [18] and ImageNet [30] datasets. We trained VQVAEs with the original formulation, referred to as KmeansVQ, and our proposed hyperbolic formulation, termed as HyperVQ, for varying numbers of codebook vectors K . The reconstruction results are presented in Tab. 1. By comparing the reconstruction mean squared error (MSE) of the two methods, we

Table 1: Comparison of reconstruction mean squared error (MSE) for KmeansVQ and HyperVQ on Cifar100 and ImageNet datasets for different codebook sizes, K .

	Cifar100 (32×32) ↓			ImageNet (128×128) ↓		
K	512	256	128	512	256	128
KmeansVQ	0.264	0.264	0.250	0.175	0.199	0.225
HyperVQ	0.216	0.241	0.256	0.175	0.202	0.217

observed that our proposed method performs on par with the original formulation. Following this, we trained a generative 15-layer GatedPixelCNN [24] model using the quantized representations obtained from VQVAE models trained on the ImageNet dataset with $K = 512$ codebook vectors for 50 epochs.

Table 2: Generative modeling performance of GatedPixelCNN with VQVAE quantized representations on ImageNet, comparing HyperVQ and the original formulation in terms of Fréchet Inception Distance (FID) and Inception Score (IS)

	FID ↓	IS ↑
KmeansVQ	143.78	5.50 ± 0.07
HyperVQ	130.31	5.77 ± 0.05

As shown in Tab. 2, HyperVQ demonstrates superior generative modeling performance compared to the original formulation, measured by the Fréchet Inception Distance (FID) [13] and Inception Score (IS) [31]. Additionally, Fig. 4a displays some reconstructions achieved with HyperVQ on the ImageNet validation set (128×128), while Fig. 4b presents samples generated by the GatedPixelCNN model.

5.3 Image Classification

To substantiate our claim that HyperVQ learns a more disentangled representation, thereby enhancing discriminative performance, we conducted experiments on the Cifar100 dataset. In these experiments, we initially trained VQVAEs with various quantization methods and a varying number of codebook vectors, K . Subsequently, we employed the pre-trained VQVAE as a feature extractor and trained a lightweight classifier atop it, as detailed in Sec. 4.3. The goal of this experiment is to show the effectiveness of HyperVQ embeddings and not to achieve state-of-the-art accuracy.

For this experiment, in addition to KmeansVQ and HyperVQ, we also included GumbelVQ for comparison. All models underwent training for 500 epochs, utilizing the same settings as described in Sec. 5.1.

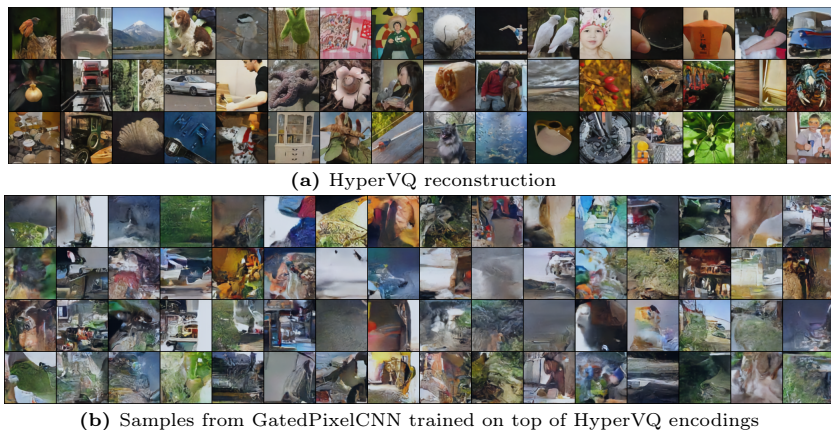


Fig. 4: Image reconstruction and generative modeling results on ImageNet.

Table 3: Evaluation of discriminative performance using pre-trained encoder and quantizer of a VQVAE as feature extractors on the Cifar100 test set.

K	512	256	128	64
KmeansVQ	30.04	29.54	30.23	29.58
GumbelVQ	25.99	26.93	26.94	27.45
HyperVQ	31.59	31.06	30.63	30.14

Table 4: Evaluation of codebook usage of the different quantization methods, as measured by average perplexity over the Cifar100 test set.

	Perplexity ($K = 512$)
KmeansVQ	58.09
GumbelVQ	169.59
HyperVQ	220.22

The results presented in Tab. 3 indicate that HyperVQ consistently outperforms other methods in terms of classification accuracy, irrespective of the number of codebook vectors.

To gain insights into the reasons behind this improved performance, we visualize the codebook vectors learned by different methods in Fig. 5 and compare the codebook usage for reconstruction based on the perplexity on the test set, as shown in Tab. 4. We treat the codebook vector as a latent representation with 1×1 spatial dimensions and decode it using the corresponding pretrained VQVAE decoder for visualization purposes.

Insights drawn from the codebook visualization and perplexities yield several interesting observations. Firstly, it is evident that KmeansVQ exhibits low codebook usage, as illustrated in Fig. 5a, where a substantial portion of the codebook vectors appears to be invalid and unused. While GumbelVQ demonstrates higher codebook usage compared to KmeansVQ and learns valid codebook vectors, the vectors themselves lack strong discriminative qualities. This limitation stems from their optimization for reconstruction, leading to some redundancy in the codebook visualizations (Fig. 5b), ultimately resulting in lower classification accuracy compared to KmeansVQ.

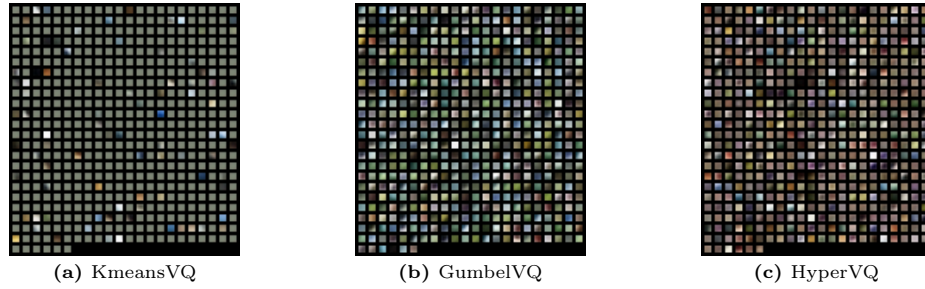


Fig. 5: Visualization of the codebook vectors for VQVAE trained on Cifar100 with different quantization methods for $K = 512$.

Contrastingly, the codebook vectors learned by HyperVQ exhibit both the highest perplexity (Tab. 4) and less redundancy (Fig. 5c). This characteristic enhances the discriminative ability of the quantized embeddings, translating into the highest classification accuracy among the methods considered.

Disentanglement and Cluster Quality To assess whether HyperVQ is capable of learning a more disentangled representation, we trained a HyperVQVAE model on the simple MNIST dataset. We maintained the latent dimension as 3, with 16 codebook vectors, for easy visualization without any post-processing. For comparison, we also trained a KmeansVQVAE model with the same configuration. To facilitate visualization, we sampled 1000 embeddings and plotted them against 3 codebook vectors each for HyperVQ and KmeansVQ.

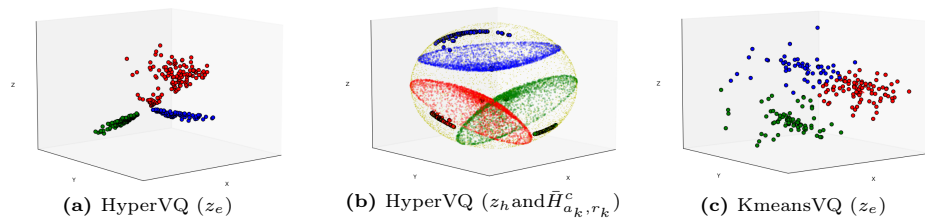


Fig. 6: Visualization and comparison of the embeddings learnt by the KmeansVQVAE and HyperVQVAE models on MNIST dataset. Fig. 6a shows the pre-projection Euclidean embeddings learnt by the HyperVQ, and Fig. 6b shows the projected embeddings along with the decision hyperplanes. Fig. 6c shows the embeddings learnt by the KmeansVQ model,

As depicted in Fig. 6, the clusters of the HyperVQVAE are more compact and disentangled than those of the VQVAE. This phenomenon arises because the hyperbolic MLR formulation encourages embeddings to be highly localized within the regions enclosed by the decision hyperplanes, thus inducing implicit disentanglement of the latent space.

Table 5: Cluster quality and robustness assessment under standard and noisy conditions, comparing Silhouette score and Davies-Bouldin Index for KmeansVQ and HyperVQ.

	Standard Conditions		Noisy Conditions	
	Silhouette Score \uparrow	DB Index \downarrow	Silhouette Score \uparrow	DB Index \downarrow
KmeansVQ	0.487	0.732	0.310	0.915
HyperVQ	0.565	0.553	0.564	0.560

Apart from the visualization, we also performed cluster quality assessment by computing the Silhouette score [28] and Davies-Bouldin Index [6]. To test the robustness, we applied random noise in the form of random rotations, flip, and gaussian noise and computed the above scores. From Tab. 5, we can see that HyperVQ is more robust towards noisy inputs and maintains its cluster compactness even under noisy conditions and in general performs better than KmeansVQ.

5.4 Quality Independent Representation Learning

We also applied HyperVQ to the VQ-SA model [36]. This model introduces a VQ layer and a self-attention layer, combining quantized and unquantized features before the final classifier of a pretrained backbone network. This augmentation aims to enhance robustness to corruptions by learning quality-independent features. The VQ-SA model undergoes training on the ImageNet dataset, incorporating corruptions from the ImageNet-C dataset [12] for data augmentation. In the original work, they employed $K = 10000$ and trained for 300 epochs. In our case, to conserve computational resources, we used $K = 1024$ and trained for 50 epochs. We also trained the original VQ-SA model under the same settings for fair comparison. Classification accuracy is reported on the clean valida-

Table 6: Classification accuracy on ImageNet and ImageNet-C for the VQ-SA method with different quantization methods.

	Clean \uparrow	Known \uparrow	Unknown \uparrow	mCE \downarrow
ResNet50	75.704	37.39	48.94	76.43
VQ-SA	70.178	58.64	53.55	52.65
HyperVQ-SA	74.344	62.30	56.09	47.61

tion set of ImageNet, along with accuracy on known and unknown corruptions in the ImageNet-C dataset. Additionally, we report the mean corruption error (mCE) [12]. From the Tab. 6, we can see that the hyperVQ-SA method significantly outperforms the original VQ-SA

5.5 Ablation Study

We conducted an ablation study to understand the individual and combined impacts of the hyperbolic Multinomial Logistic Regression (MLR) formulation and the use of the representative point on the decision hyperplane as the codebook vector in our proposed method.

Our evaluation compared the performance of our HyperVQ method against traditional vector quantization approaches such as KmeansVQ and GumbelVQ, as well as two variants designed for this study: HyperKmeansVQ, which uses codebook vectors in hyperbolic space learned with the KmeansVQ mechanism and distances induced by the Poincaré ball model; and HyperEmbMatVQ, which applies the hyperbolic MLR formulation but uses the embedding matrix as the codebook vectors, similar to GumbelVQ but with logits derived from the hyperbolic MLR.

The findings from our study, as depicted in Table 7, highlight the benefits of incorporating the hyperbolic MLR formulation with the embedding matrix, which notably improves classification accuracy over the GumbelVQ model. Additionally, leveraging the representative point on the decision hyperplane as the codebook vector further enhances classification performance, establishing our HyperVQ method as the superior approach among those tested.

6 Limitations and Conclusion

We proposed an alternative formulation for vector quantization utilizing hyperbolic space, demonstrating its effectiveness in enhancing the discriminative power of quantized embeddings while preserving the generative capabilities of the VQ-VAE. The hyperbolic MLR formulation was shown to encourage a more compact representation in the pre-quantized Euclidean latent space. Through various experiments, we illustrated that HyperVQ can serve as a drop-in replacement for multiple methods across domains, improving their performance.

However, it is important to note that the projections to and from the hyperbolic space exhibit sensitivity to numerical instability, particularly near the boundary of the Poincaré ball. This sensitivity raises concerns, especially when employing low-precision methods, such as 16-bit floating-point numbers, during model training, as it may lead to instability. Consequently, this limitation could restrict the application of HyperVQ in very large models, which are typically trained using low or mixed precision. Further analysis of the stability of HyperVQ under low-precision training is left for future work.

Table 7: Comparison of Classification Accuracy on CIFAR-100 for various vector quantization methods with a codebook size of 512.

	Accuracy (%)
KmeansVQ	30.04
HyperKmeansVQ	22.42
GumbelVQ	25.99
HyperEmbMatVQ	28.28
HyperVQ	31.59

7 Acknowledgements

This work was partially supported by JST Moonshot R&D Grant Number JP-MJPS2011, CREST Grant Number JPMJCR2015 and Basic Research Grant (Super AI) of Institute for AI and Beyond of the University of Tokyo.

References

1. Atigh, M.G., Schoep, J., Acar, E., Van Noord, N., Mettes, P.: Hyperbolic image segmentation. In: Proceedings of the IEEE/CVF conference on computer vision and pattern recognition. pp. 4453–4462 (2022) [2](#), [3](#)
2. Baevski, A., Schneider, S., Auli, M.: vq-wav2vec: Self-supervised learning of discrete speech representations. In: International Conference on Learning Representations (2020), <https://openreview.net/forum?id=rylwJxrYDS> [2](#), [3](#), [6](#), [7](#)
3. Baevski, A., Zhou, Y., Mohamed, A., Auli, M.: wav2vec 2.0: A framework for self-supervised learning of speech representations. *Advances in neural information processing systems* **33**, 12449–12460 (2020) [2](#), [3](#)
4. Bengio, Y., Léonard, N., Courville, A.C.: Estimating or propagating gradients through stochastic neurons for conditional computation. *CoRR* **abs/1308.3432** (2013) [2](#), [6](#), [7](#)
5. Crowson, K., Biderman, S., Kornis, D., Stander, D., Hallahan, E., Castricato, L., Raff, E.: Vqgan-clip: Open domain image generation and editing with natural language guidance. In: European Conference on Computer Vision. pp. 88–105. Springer (2022) [3](#)
6. Davies, D.L., Bouldin, D.W.: A cluster separation measure. *IEEE Transactions on Pattern Analysis and Machine Intelligence* **PAMI-1**(2), 224–227 (1979). <https://doi.org/10.1109/TPAMI.1979.4766909> [13](#)
7. Desai, K., Nickel, M., Rajpurohit, T., Johnson, J., Vedantam, S.R.: Hyperbolic image-text representations. In: International Conference on Machine Learning. pp. 7694–7731. PMLR (2023) [3](#)
8. Esser, P., Rombach, R., Ommer, B.: Taming transformers for high-resolution image synthesis. In: Proceedings of the IEEE/CVF conference on computer vision and pattern recognition. pp. 12873–12883 (2021) [3](#)
9. Ganea, O., Bécigneul, G., Hofmann, T.: Hyperbolic neural networks. *Advances in neural information processing systems* **31** (2018) [3](#), [4](#), [5](#), [6](#)
10. Gray, R.: Vector quantization. *IEEE ASSP Magazine* **1**(2), 4–29 (1984). <https://doi.org/10.1109/MASSP.1984.1162229> [2](#)
11. Gu, S., Chen, D., Bao, J., Wen, F., Zhang, B., Chen, D., Yuan, L., Guo, B.: Vector quantized diffusion model for text-to-image synthesis. In: Proceedings of the IEEE/CVF Conference on Computer Vision and Pattern Recognition. pp. 10696–10706 (2022) [3](#)
12. Hendrycks, D., Dietterich, T.: Benchmarking neural network robustness to common corruptions and perturbations. *Proceedings of the International Conference on Learning Representations* (2019) [13](#)
13. Heusel, M., Ramsauer, H., Unterthiner, T., Nessler, B., Hochreiter, S.: Gans trained by a two time-scale update rule converge to a local nash equilibrium. *Advances in neural information processing systems* **30** (2017) [10](#)
14. Jang, E., Gu, S., Poole, B.: Categorical reparameterization with gumbel-softmax. In: International Conference on Learning Representations (2017), <https://openreview.net/forum?id=rkE3y85ee> [7](#)

15. Khrukov, V., Mirvakhabova, L., Ustinova, E., Oseledets, I., Lempitsky, V.: Hyperbolic image embeddings. In: Proceedings of the IEEE/CVF Conference on Computer Vision and Pattern Recognition. pp. 6418–6428 (2020) [2](#), [3](#)
16. Kingma, D.P., Ba, J.: Adam: A method for stochastic optimization. arXiv preprint arXiv:1412.6980 (2014) [9](#)
17. Kochurov, M., Karimov, R., Kozlukov, S.: Geoopt: Riemannian optimization in pytorch (2020) [9](#)
18. Krizhevsky, A.: Learning multiple layers of features from tiny images. Master’s thesis, Department of Computer Science, University of Toronto (2009) [9](#)
19. Łańcucki, A., Chorowski, J., Sanchez, G., Marxer, R., Chen, N., Dolfing, H.J., Khurana, S., Alumäe, T., Laurent, A.: Robust training of vector quantized bottleneck models. In: 2020 International Joint Conference on Neural Networks (IJCNN). pp. 1–7. IEEE (2020) [3](#)
20. Lou, A., Katsman, I., Jiang, Q., Belongie, S., Lim, S.N., De Sa, C.: Differentiating through the fréchet mean. In: International Conference on Machine Learning. pp. 6393–6403. PMLR (2020) [7](#)
21. Lu, R., Wu, Y., Tian, L., Wang, D., Chen, B., Liu, X., Hu, R.: Hierarchical vector quantized transformer for multi-class unsupervised anomaly detection. In: Thirty-seventh Conference on Neural Information Processing Systems (2023), <https://openreview.net/forum?id=c1JTNssgn6> [3](#)
22. Mathieu, E., Le Lan, C., Maddison, C.J., Tomioka, R., Teh, Y.W.: Continuous hierarchical representations with poincaré variational auto-encoders. Advances in neural information processing systems **32** (2019) [3](#)
23. Nickel, M., Kiela, D.: Poincaré embeddings for learning hierarchical representations. Advances in neural information processing systems **30** (2017) [2](#), [3](#)
24. Van den Oord, A., Kalchbrenner, N., Espeholt, L., Vinyals, O., Graves, A., et al.: Conditional image generation with pixelcnn decoders. Advances in neural information processing systems **29** (2016) [3](#), [10](#)
25. Paszke, A., Gross, S., Massa, F., Lerer, A., Bradbury, J., Chanan, G., Killeen, T., Lin, Z., Gimelshein, N., Antiga, L., Desmaison, A., Kopf, A., Yang, E., DeVito, Z., Raison, M., Tejani, A., Chilamkurthy, S., Steiner, B., Fang, L., Bai, J., Chintala, S.: Pytorch: An imperative style, high-performance deep learning library. In: Advances in Neural Information Processing Systems 32, pp. 8024–8035. Curran Associates, Inc. (2019), <http://papers.neurips.cc/paper/9015-pytorch-an-imperative-style-high-performance-deep-learning-library.pdf> [9](#)
26. Peng, W., Varanka, T., Mostafa, A., Shi, H., Zhao, G.: Hyperbolic deep neural networks: A survey. IEEE Transactions on pattern analysis and machine intelligence **44**(12), 10023–10044 (2021) [2](#), [3](#)
27. Petermann, D., Wichern, G., Subramanian, A., Le Roux, J.: Hyperbolic audio source separation. In: ICASSP 2023-2023 IEEE International Conference on Acoustics, Speech and Signal Processing (ICASSP). pp. 1–5. IEEE (2023) [2](#), [3](#)
28. Rousseeuw, P.J.: Silhouettes: A graphical aid to the interpretation and validation of cluster analysis. Journal of Computational and Applied Mathematics **20**, 53–65 (1987). [https://doi.org/https://doi.org/10.1016/0377-0427\(87\)90125-7](https://doi.org/https://doi.org/10.1016/0377-0427(87)90125-7), <https://www.sciencedirect.com/science/article/pii/0377042787901257> [13](#)
29. Roy, A., Vaswani, A., Neelakantan, A., Parmar, N.: Theory and experiments on vector quantized autoencoders. CoRR **abs/1805.11063** (2018) [3](#)
30. Russakovsky, O., Deng, J., Su, H., Krause, J., Satheesh, S., Ma, S., Huang, Z., Karpathy, A., Khosla, A., Bernstein, M., Berg, A.C., Fei-Fei, L.: Imagenet large scale visual recognition challenge. International Journal of Computer Vision (IJCV) **115**(3), 211–252 (2015) [9](#)

31. Salimans, T., Goodfellow, I., Zaremba, W., Cheung, V., Radford, A., Chen, X.: Improved techniques for training gans. *Advances in neural information processing systems* **29** (2016) [10](#)
32. Shimizu, R., Mukuta, Y., Harada, T.: Hyperbolic neural networks++. In: *International Conference on Learning Representations* (2021), <https://openreview.net/forum?id=Ec85b0tUwbA> [3](#), [5](#), [9](#)
33. Skopek, O., Ganea, O.E., Bécigneul, G.: Mixed-curvature variational autoencoders. In: *8th International Conference on Learning Representations (ICLR 2020)(virtual)*. *International Conference on Learning Representations* (2020) [3](#)
34. Takida, Y., Shibuya, T., Liao, W., Lai, C.H., Ohmura, J., Uesaka, T., Murata, N., Takahashi, S., Kumakura, T., Mitsufuji, Y.: Sq-vae: Variational bayes on discrete representation with self-annealed stochastic quantization. *arXiv preprint arXiv:2205.07547* (2022) [3](#)
35. Van Den Oord, A., Vinyals, O., et al.: Neural discrete representation learning. *Advances in neural information processing systems* **30** (2017) [1](#), [3](#)
36. Yang, Z., Dong, W., Li, X., Huang, M., Sun, Y., Shi, G.: Vector quantization with self-attention for quality-independent representation learning. In: *Proceedings of the IEEE/CVF Conference on Computer Vision and Pattern Recognition*. pp. 24438–24448 (2023) [2](#), [3](#), [13](#)
37. Zeghidour, N., Luebs, A., Omran, A., Skoglund, J., Tagliasacchi, M.: Soundstream: An end-to-end neural audio codec. *IEEE/ACM Transactions on Audio, Speech, and Language Processing* **30**, 495–507 (2021) [1](#), [3](#)